



EARLY CRUSTAL EVOLUTION OF MARS¹

Francis Nimmo

*Department of Earth and Space Sciences, University of California,
Los Angeles, California 90095-1567; email: nimmo@ess.ucla.edu*

Ken Tanaka

United States Geological Survey, Flagstaff, Arizona 86001; email: ktanaka@usgs.gov

Key Words gravity, topography, magnetism, geology, comparative planetology

■ **Abstract** The bulk of the ~50-km-thick Martian crust formed at ~4.5 Gyr B.P., perhaps from a magma ocean. This crust is probably a basaltic andesite or andesite and is enriched in incompatible and heat-producing elements. Later additions of denser basalt to the crust were volumetrically minor, but resurfaced significant portions of the Northern hemisphere. A significant fraction of the total thickness of the crust was magnetized prior to 4 Gyr B.P., with the magnetization later selectively removed by large impacts. Early large impacts also modified the hemispheric contrast in crustal thickness (the dichotomy), which was possibly caused by long-wavelength mantle convection. Subsequent Noachian modification of the crust included further impacts, significant fluvial erosion, and volcanism associated with the formation of the Tharsis rise. Remaining outstanding questions include the origin of the dichotomy and the nature of the magnetic anomalies.

INTRODUCTION

Mars is in some ways the type example of a terrestrial planet. It is neither geologically stillborn, like Mercury or the Moon, nor so active that most of the geological record has been destroyed, like Venus or the Earth. The prolonged geological evolution of Mars is recorded in the physical and chemical characteristics of its crust. This article summarizes our current understanding of the characteristics of the Martian crust, and its implications for the evolution of Mars and the other terrestrial planets. Because the bulk of the Martian crust formed early, we focus on events in roughly the first billion years of the planet's history.

We first summarize the characteristics of the crust as it appears at the present day before discussing the manner in which the early crust may have formed. We then describe how this crust was modified subsequent to its formation, and conclude

¹The U.S. Government has the right to retain a nonexclusive, royalty-free license in and to any copyright covering this paper.

3.2 NIMMO ■ TANAKA

with a summary and a list of questions that we hope will be answered in the future. We focus on the bulk properties of the crust and pay relatively little attention to surficial processes such as erosion and sedimentation. Our conclusions are based primarily on the results of the Mars Global Surveyor (MGS) mission (Albee et al. 2001), though where appropriate we also draw on the results from Pathfinder (Golombek et al. 1997) and Mars Odyssey (Saunders et al. 2004); at the time of writing, only preliminary results from the two Mars Exploration Rovers (MERs) (Suyres et al. 2004) are available. Because future NASA missions are likely to focus on near-subsurface and atmospheric phenomena, we think it unlikely that such missions will greatly change our conclusions. Two exceptions would be if Martian seismometers are ever successfully deployed, or if appropriate Martian samples are returned to Earth.

The Martian crust has been the subject of many previous surveys. The state of knowledge at the end of the Viking missions was captured in the book *Mars* (Kieffer et al. 1992). A more recent compendium on crustal chronology and geochemistry is provided by Kallenbach et al. (2001), and a lucid summary of the Martian crust is given by Zuber (2001). An article similar in scope to this one is by S.C. Solomon, O. Aharonson, J.M. Aurnou, W.B. Banerdt, M.H. Carr, et al. (submitted manuscript).

CHARACTERISTICS OF THE ANCIENT CRUST

At present, all terrestrial planets consist of three main layers: (*a*) an innermost iron core, surrounded by (*b*) a silicate mantle, and topped with a thin layer, chemically distinct from the underlying mantle, known as (*c*) the crust. The silicate interior of most planets is likely to be convecting, but there usually exists a cold, near-surface layer that does not take part in convection and is called the lithosphere. The lithosphere usually contains the entire crust and part of the underlying mantle, and is a mechanical rather than a chemical layer.

Outcrop/Subcrop

Crustal rocks on Mars have been subdivided according to age on the basis of geologic mapping relations and impact crater densities that define and describe three major periods of the planet's geologic history (Scott & Carr 1978, Scott et al. 1986–1987, Tanaka 1986) (Figure 1, see color insert). The oldest exposed rocks that comprise most of the ancient southern highlands formed during the Noachian Period (Figure 2). Noachian rocks are partly buried by younger Hesperian and Amazonian (youngest) materials in the northern lowlands, at the Tharsis and Elysium volcanic rises, in Hellas and Argyre basins, and in other scattered localities. Furthermore, Noachian materials appear to be underlain by older, “pre-Noachian” material, whose presence is indicated by high densities of impact craters tens to hundreds of kilometers in diameter (Frey 2002; see below). Collectively, “pre-Noachian” and Noachian rocks comprise the early Martian crust.

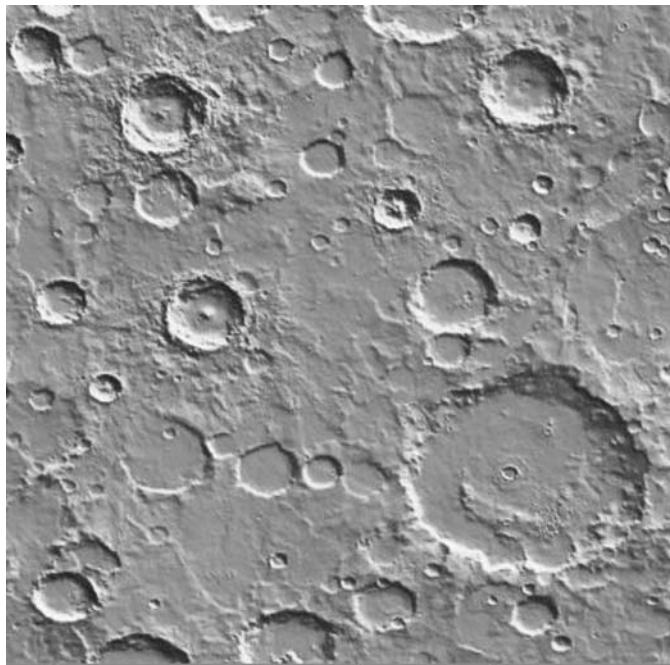


Figure 2 Part of Noachis Terra, Mars, the type area for material of the Noachian Period (Scott & Carr 1978). Shaded-relief view from MOLA topography, illuminated from upper right; centered at 44°S, 16°E; image width is 600 km.

Age

Impact crater size-frequency distributions provide a statistical tool for determining relative ages of Martian surfaces. Inferring absolute ages on the basis of crater densities requires knowledge of the cratering rate. The cratering rate for Mars has been estimated primarily in comparison to lunar cratering and the population of Mars-crossing asteroids (Hartmann 1978, Ivanov 2001, Hartmann & Neukum 2001). These dating methods are imprecise, especially for younger Hesperian and Amazonian surfaces for which ages may be in error by a factor of 2 to 3 (Hartmann & Neukum 2001). For ages during the Noachian, however, these authors as well as Tanaka (1986) and Frey (2004) are in close agreement and conclude that the Late Noachian ranges from 3.7 to 3.82 Ga, the Middle Noachian is from 3.82 to 3.93 Ga, and the Early Noachian is >3.93 Ga (Figure 3).

High-resolution topography collected by MGS has allowed the identification of quasi-circular depressions (QCDs), interpreted as ancient buried impact basins. Frey (2004) has identified ~560 QCDs > 200 km in diameter. Assuming a -2 power law distribution and the Hartmann & Neukum (2001) cratering chronology, Frey (2004) derived absolute surface ages on the basis of QCD densities (Figure 3).

3.4 NIMMO ■ TANAKA

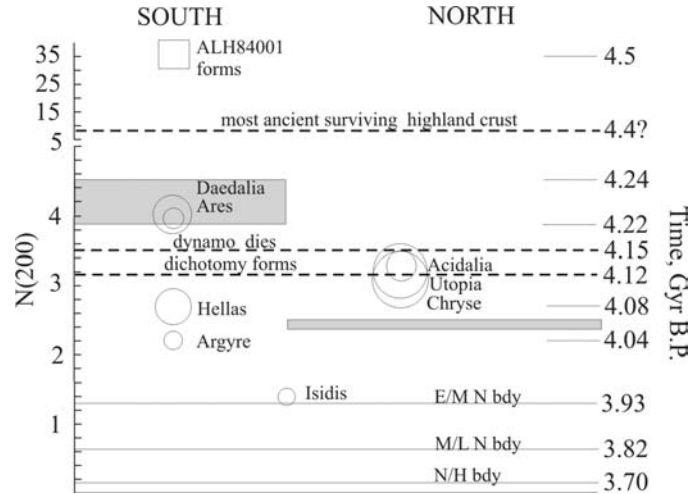


Figure 3 Timeline of events in early Martian history. Left-hand scale is number of craters exceeding 200 km in diameter per million square km; data from Frey (2004). Note change in interval at $N(200) = 5$. Right-hand scale is time from Hartmann & Neukum (2001, Figure 14), assuming a -2 power law crater size distribution. The formation of the dichotomy and the death of the dynamo probably overlapped in time. Circles are impact basins, scaled to basin size; shaded areas denote crater density range for buried and total crust (Frey 2004) and place lower bound on basement age. Solid lines depict stratigraphic boundaries, dashed lines depict major events. See text for a discussion of this timescale.

These model ages are consistent with geologic relations in which better-preserved, large impact basins postdate more degraded basins and the northern plains. The oldest exposed rocks include the Hellas basin rim material (4.08 ± 0.06 Ga). The basement of the northern plains may have formed $\sim 4.12 \pm 0.08$ Ga and the signature of buried highland crust may extend back to $\sim 4.2 \pm 0.1$ Ga. Geologic periods are defined on the age range of representative rocks. Thus for Mars, the oldest exposed rocks form the base of the Noachian; the defining event for the beginning of the Noachian is the Hellas impact (Frey 2004); earlier structures including the northern lowlands and many QCDs are thus “pre-Noachian”.

Geomorphology and Geologic History

The distribution of geologic materials and structures across Mars shows dramatic regional variations (Figure 1). For the most part, the geologic history of Mars can be described in the context of highland, lowland, and volcano-tectonic regions. Generalized geologic units (adapted largely from Scott et al. 1986–87 and Tanaka et al. 1988, 1992, 2003b) expressing this history are shown in Figure 1 and italicized below. Here we focus primarily on the exposed Noachian rocks.

Rocks of the predominantly Noachian southern highlands cover half the planet and have a rugged relief resulting largely from impact craters and basins (Figure 2). The oldest exposed materials of Early Noachian (EN) age form massifs and other high-relief terrains that include the rim materials (*EN massif material*) of Hellas, Argyre, and Isidis basins, and the putative Chryse basin (Schultz et al. 1982). Noachian materials (*N materials*) that make up rugged, highly cratered, commonly layered terrains in highland regions embay EN massif material and include mixtures of deposits of impact, sedimentary, and volcanic origins (Tanaka et al. 1992, Tanaka 2000, Malin & Edgett 2000, Hynek & Phillips 2001). Relatively thin sedimentary and/or volcanic deposits overlying N materials form scattered outcrops in intercrater plains (*LN-EH materials*) and possibly include paleolake deposits (Irwin & Howard 2002, Irwin et al. 2002). Precipitation and runoff may account for the higher rates of highland erosion during the Noachian (Craddock & Maxwell 1993, Craddock & Howard 2002). Sill intrusion may also melt ground ice, leading to discharges and chaos formation in some intercrater plains (Wilhelms & Baldwin 1989). Along the slopes of the lowland boundary and interior of Argyre basin, Noachian materials were degraded into knobs and plains deposits during the Late Noachian and into the Hesperian (*LN-EH knobby materials*). Throughout the Noachian and into the Hesperian, contractional ridges developed, with wrinkled crenulations apparent in some smoother plains (Tanaka et al. 1991, Watters 1993, Mueller & Golombek 2004). Some horizontal scarps that ring the northern lowlands and Hellas basin have been proposed to be paleoshorelines (Clifford & Parker 2001, Moore & Wilhelms 2001); if correct, these shorelines would indicate large volumes of water on Mars during the Noachian and perhaps into the Hesperian.

The vast northern plains covering nearly one third of the planet show little exposure of Noachian-age materials, owing to Hesperian and Amazonian resurfacing (Figure 1). The oldest materials within the lowlands form high-standing outcrops of mostly knobby, cratered terrain where Elysium, Amazonis, and Arcadia Planitiae come together as well as a large mesa in Acidalia Planitia (*LN-EH knobby* and *N materials*). Gently sloping plains made up of *H materials* along the highland margin that grade with LN-EH knobby materials appear to result from mass wasting and erosion and perhaps mud volcanism (Tanaka et al. 2003a,b). Subsequent widespread as well as local resurfacing of the lowlands occurred because of deposition caused by catastrophic outflow events (Carr 1979, MacKinnon & Tanaka 1989), volcanism (Greeley & Spudis 1981), and aeolian and periglacial processes. Emplacement of a widespread, early Amazonian deposit in the lowlands below −3500 to −4000 m elevation (the *EA Vastitas Borealis unit*) may have been the result of ocean (Parker et al. 1989) or debris-flow (Tanaka et al. 2001) deposition.

Mars appears to have been volcanically active throughout its preserved geologic history. Early to Middle Noachian volcanic features are difficult to identify conclusively because of subsequent degradation by impacts. *EN massif materials* and *N-EH volcanic material* make up highly fractured, rugged materials in western Tempe Terra and the western/southwestern Thaumasia highlands, and are

3.6 NIMMO ■ TANAKA

probably volcanic (Dohm et al. 2001, Moore 2001). During the Late Noachian and into the Early Hesperian, volcanism continued at the Tharsis rise (see Tharsis, below), emplacing *N-EH volcanic materials*, although much of this record is likely buried by younger rocks. Later volcanism was confined mainly to the Elysium and Tharsis rises. Globally, the volcanic resurfacing quantified by Tanaka et al. (1988) probably peaked during the Early Hesperian; based on the timescale of Hartmann & Neukum (2001), the global median age of volcanic material is 3.5 Ga.

Physical Characteristics

The physical characteristics of the crust, such as thickness, density, and rigidity, provide important constraints on its composition and mode of formation. Useful summaries of likely characteristics are provided by Wiczorek & Zuber (2004) and Neumann et al. (2004).

Of the various physical properties of interest, perhaps the easiest to constrain is the near-surface crustal density. At sufficiently short wavelengths, the gravitational attraction caused by topography depends only on the topographic amplitude and the surface density (e.g., Nimmo 2002). The ratio of gravity to topography, known as the admittance, increases with decreasing wavelength, at a rate depending on the elastic rigidity of the lithosphere. At short wavelengths, the admittance reaches a constant value of $2\pi\rho G$, where G is the gravitational constant and ρ is the surface density. Since both the gravity field and the topography of Mars were measured by MGS (Figure 4, see color insert), the crustal surface density can be derived by calculating the admittance.

The admittance may be calculated in one of two ways: either directly from observations of the line-of-sight (LOS) spacecraft acceleration (e.g., McKenzie et al. 2002) or from the spherical harmonic gravity field derived from the LOS observations (e.g., McGovern et al. 2002). For Mars, both techniques produce broadly similar results. McGovern et al. (2004) investigated three areas of the southern highlands and found surface densities in the range of 2500 to 3000 kg m⁻³ and variable degrees of subsurface loading. Nimmo (2002) looked at an area straddling the dichotomy and obtained a surface density of 2500 kg m⁻³. McKenzie et al. (2002) investigated the entire highlands south of 20°S but were unable to obtain a reliable density estimate.

The surface densities obtained for the Noachian crust are generally less than the well-constrained surface densities of the Tharsis volcanoes of 3100 ± 200 kg m⁻³ (McKenzie et al. 2002, Turcotte et al. 2002, McGovern et al. 2004). They are also lower than the densities of Martian meteorites, typically 3200 to 3300 kg m⁻³ (Lodders 1998). The obvious conclusion is that the Noachian near-surface material is either porous (presumably due to impacts) or composed of low-density sediments. A two-layer crustal model, with a low-density surface layer, fits the admittance data (Nimmo 2002). Unfortunately, the thickness of the near-surface layer is poorly constrained by the data. Other arguments concerning the porosity structure of the Martian crust rely on studies of the grain-size distributions of

impacted terrestrial materials (MacKinnon & Tanaka 1989) and the structure of the lunar megaregolith (Clifford 1993). The near-surface Martian crust has probably been modified by sedimentation, erosion, and hydrous alteration, or infilling with ice subsequent to its formation.

No seismic data are available to constrain the crustal thickness. However, given an assumed mean crustal thickness, gravity and topography data can be used to find the spatial variation around this mean value. Zuber et al. (2000) used a mean value of 50 km and found a crustal thickness in the range of 3 to 92 km. A smaller mean thickness would result in negative values beneath the large impact basins; Wieczorek & Zuber (2004) and Neumann et al. (2004) used this argument to find a lower bound on the mean crustal thickness of 32 and 45 km, respectively. Note that these models assume a constant crustal density, although Spohn et al. (2001) point out that lateral variations in density could also account for significant topographic variations. Both Zuber et al. (2000) and Nimmo & Stevenson (2001) argued that crustal thicknesses in excess of ~ 100 km would lead to the destruction of lateral crustal thickness variations by lower crustal flow, giving an upper limit on crustal thickness.

It is theoretically possible to use the admittance technique to infer the crustal thickness, but uncertainties in the rigidity of the lithosphere, the fraction of subsurface loading, and the density of the crust make such an approach imprecise. McGovern et al. (2002) obtained values of $50(+12, -42)$ km for Noachis Terra, and Nimmo (2002) found a mean crustal thickness of <75 km in the area investigated. Turcotte et al. (2002) obtained a mean crustal thickness around the Hellas basin of 90 ± 10 km using a spatial rather than a spectral approach. Wieczorek & Zuber (2004) showed that this approach introduces errors, and they derived a mean crustal thickness for the southern highlands of 57 ± 24 km. Crustal thicknesses have also been estimated using geochemical data (see Chemical Characteristics, below).

Because the lithosphere is cold, it retains appreciable elastic strength over geological periods. This overall rigidity is important, because it can be used to constrain the heat flux, and is often expressed as an effective elastic thickness T_e (typically two to four times smaller than the lithospheric thickness). The value of T_e recorded is generally relevant to the time of loading, and not to the present day. Elastic thickness estimates for Noachian age areas include <16 km (McGovern et al. 2004) and 15 km (McKenzie et al. 2002). The inferred heat fluxes are >35 mW m⁻² and 50 mW m⁻², respectively. These heat fluxes assume a linear temperature gradient, which may not be correct if significant fractions of heat-producing elements are concentrated in the crust (McLennan 2001). Furthermore, T_e estimates may be biased if subsurface loading is not taken into account (Nimmo 2002). Nonetheless, it is shown below that these heat flux estimates are compatible with geochemical predictions (see Summary).

The magnetic field of Mars may be measured either directly, with a vector magnetometer, or indirectly, with an electron reflectometer (Mitchell et al. 2001). Both techniques are limited in resolution by the spacecraft altitude; as a result,

3.8 NIMMO ■ TANAKA

magnetic anomalies at wavelengths less than ~ 200 km cannot be detected. One of the biggest surprises of the MGS mission was the detection of large, localized magnetic anomalies, principally in areas with Noachian surface ages (Acuna et al. 1999, Connerney et al. 1999). Mars does not possess a global, principally dipolar magnetic field at the present day; the local anomalies, however, suggest that it did possess such a field in the past. Figure 4*b* presents a spherical harmonic representation of the data from the model of Purucker et al. (2000); several other workers (Connerney et al. 2001, Cain et al. 2003, Arkani-Hamed 2002) have produced essentially identical results. All the largest anomalies occur in the southern highlands, and the large impact basins (Utopia, Hellas, Argyre, and Isidis) are almost free of magnetic anomalies. However, a few weak anomalies are found in the northern lowlands (e.g., Hood & Zakharian 2001) and in the areas west of Tharsis (Johnson & Phillips 2004).

Because the large impact basins Hellas and Argyre have essentially no magnetic anomalies, Acuna et al. (1999) concluded that the global field must have ceased before these basins formed. Furthermore, the apparent correlation of large impact basins with an absence of magnetic anomalies suggests that the impact events removed any pre-existing anomalies. Therefore, the global dynamo must have ended before the formation of the large impact basins. Weiss et al. (2002) and Antretter et al. (2003) showed that the Martian meteorite ALH84001 acquired its magnetization between 3.9 and 4.1 Gyr B.P. Because this magnetization may have been acquired by crystallizing in a local magnetic field caused by pre-existing crustal anomalies, the dynamo could have existed at any time prior to this date. This observation suggests that the argument of Schubert et al. (2000) for a late-onset (< 4 Gyr B.P.) dynamo is probably not correct.

The apparent absence of magnetization in most of the northern plains is puzzling. A uniformly magnetized crust, or one with short-wavelength anomalies, would not be detectable, but it is unclear why either situation should occur. The observations of Frey (2004) suggest that little (~ 100 Myr) time elapsed between the formation of the southern highlands and the northern lowlands basement. It seems unlikely that the dynamo ceased within this narrow time interval, especially as there are patches of magnetized crust in the north. Subsequent hydrothermal demagnetization of the northern crust is possible (S.C. Solomon, O. Aharonson, J.M. Aurnou, W.B. Banerdt, M.H. Carr, et al., submitted manuscript), but would require enormous volumes of water to penetrate several tens of kilometers deep (compare with Harrison & Grimm 2002). One possibility is that the northern lowlands are mostly demagnetized because of early, large impacts, such as that which formed the Utopia basin (Figure 4). The giant impact hypothesis is discussed further below (see Hemispheric Dichotomy).

The lack of magnetization in the areas centered on the large impact basins has been ascribed to some combination of excavation, brecciation/reorientation, shock, and thermal demagnetization (Acuna et al. 1999, Nimmo & Gilmore 2001, Hood et al. 2003, Rochette et al. 2003, Mohit & Arkani-Hamed 2004). Nimmo & Gilmore (2001) inferred a magnetization depth of 35 km, with a factor of 3 uncertainty,

on the basis of the sizes of basins which showed evidence for demagnetization. A similar value (46 km) was obtained by Voorhies et al. (2002), who used the slope of the Martian magnetic power spectrum to derive a characteristic source depth.

If the magnetization (per unit volume) of the rock is known, the thickness of the magnetized layer may thus be inferred. The amplitude of the Martian anomalies is at least one order of magnitude greater than that of terrestrial crustal magnetic anomalies, measured at the same altitude (Connerney et al. 1999). Terrestrial oceanic crustal magnetization usually extends to a depth of a few kilometers (e.g., Pariso & Johnson 1993); hence, assuming similar magnetizations for Mars, the magnetized layer is probably a few tens of kilometers thick. Of course, the magnetization per unit volume of the Martian source rocks is unknown. Oceanic and continental terrestrial basaltic rocks have maximum magnetizations of 20 to 30 A m⁻¹ (Johnson & Salem 1994, Kristjansson & Johansson 1999), which may be significantly reduced by subsequent hydrothermal alteration (Pariso & Johnson 1991). Connerney et al. (1999) required similar magnetizations to match the observations, assuming a magnetized layer thickness of 30 km.

The mineral(s) responsible for the magnetic anomalies on Mars is also unknown. Based on the oxidized, iron-rich, and roughly basaltic nature of the Martian crust, the most likely mineral(s) is titanomagnetite, hematite, titanohematite, or pyrrhotite (Kletetschka et al. 2000). Martian meteorites typically contain titanomagnetite (Weiss et al. 2002) or pyrrhotite (Rochette et al. 2001). These minerals differ in the temperature (the Curie temperature) and pressure at which they demagnetize. The intensity and the stability of the magnetization depend not only on the mineralogy but also on the grain size (Kletetschka et al. 2000, Nimmo 2000). If the mineralogy and depth of magnetization are known, the Curie temperature can be used to place a constraint on the thermal structure of the crust (see Summary, below).

One of the puzzles of the magnetic anomalies is that they show almost no correlation with any other data set (Acuna et al. 1999, Purucker et al. 2000). Apart from their overwhelming occurrence in areas with Noachian surface ages, there is no obvious relationship to topography, gravity, tectonic setting, or crustal thickness, although there is a correlation with areas containing valley networks (Harrison & Grimm 2002). This general lack of correlation also tends to support the idea of deeply buried magnetic anomalies.

A final surprise in the magnetic data was the appearance of elongated features (Connerney et al. 1999), somewhat reminiscent of the sea-floor magnetic stripes that demonstrated the existence of plate tectonics on Earth. The identification of ancient plate tectonics on Mars would be an enormously important step forward and is discussed in some detail below (see Plate Tectonics?). Here we note that the elongated features are neither as stripe-like nor as symmetrical as their terrestrial counterparts. Furthermore, their scale is quite different: The stripes are 100 to 200 km wide, much wider than most terrestrial stripes. Smaller wavelength variability may occur but would not be visible at spacecraft altitudes. Alternative interpretations of the lineations do exist. Nimmo (2000) argued that they could instead be due to

3.10 NIMMO ■ TANAKA

large-scale dike intrusion, and Fairen et al. (2002) suggested accretionary terrains during an early episode of plate tectonics.

Chemical Characteristics

The chemical composition of the crust is an important clue to its origin (see below). Basaltic crusts, such as that of Venus, the Earth's seafloor, or the lunar maria, are formed by partial melting of mantle material and have relatively low silica contents (45–52 wt %). Fractional crystallization of basaltic magmas can produce small volumes of andesites, more silica-rich melts (57–62 wt %), without requiring the presence of water (e.g., Hess 1989). The lunar highlands, which are mostly plagioclase, crystallized and floated to the top of a primordial magma ocean (Taylor 1992). The Earth's continents are also plagioclase and silica rich, but probably formed at subduction zones, where the presence of water leads to more complicated mineralogical assemblages (e.g., Hess 1989).

There is a vast array of literature on the petrology and geochemistry of the Martian crust, which can only be briefly summarized here. More in-depth summaries can be found in Nyquist et al. (2001), Wanke et al. (2001), McSween (2002), and McSween et al. (2003). Table 1 summarizes the available Martian compositional data. Below, it is argued that these data provide a reasonably consistent picture of an ancient (4.5 Gyr) crust that is enriched in rare-Earth elements (REEs), radiogenic isotopes and potassium and is somewhat more silica rich than basaltic Martian meteorites. Erupted subsequently, and overlying this crust, are smaller volumes of a basaltic material that show a depletion in light REEs.

There are three sources of information on the chemical composition of the Martian crust: Martian meteorites; in situ analyses by the two Viking missions, Mars Pathfinder (MPF) and the MERs; and remote sensing observations, especially infrared (IR), gamma-ray (GR), and neutron emission. The four main lines of evidence for the existence of a silica-rich crust are the variable REE patterns in basaltic Martian meteorites, the "soil-free rock" (SFR) composition inferred from MPF measurements, the high potassium in Martian soils compared with basaltic Martian meteorites, and mineralogical inferences from IR observations. Although each of these lines of evidence has its problems, collectively they give a reasonably coherent picture.

Although the Martian meteorites are well characterized, they do not appear to be representative of bulk Martian crustal compositions for at least three reasons. First, various isotopic systems suggest that the bulk of the crust was produced early, prior to 4 Gyr (see below), whereas the Martian meteorites are mostly young (1.3 Gyr or less) (e.g., Nyquist et al. 2001). Second, the depletion in light REEs (LREEs) in some Martian meteorites suggests that they were generated from a source from which the Martian crust had already been extracted. Finally, most Martian meteorites are cumulates (e.g., McSween 1994) and are thus hard to relate directly to either their parent magmas or the bulk crustal composition.

The timing of crustal extraction relies on the fact that pairs of radioactive parents and daughters (e.g., Rb/Sr, Sm/Nd, Lu/Hf) show different partitioning during melting. Different authors and different isotopic systems all produce the

TABLE 1 Summary of observations of Martian surface compositions

Species (wt %)	Mean basaltic sherg. ^a	Mean MPF soil ^b	Mean MER soil ^c	MPF soil-free rock ^b	Mean MER rock ^c	TES surface type 1 ^d	TES surface type 2 ^d	GRS Phobos-2 ^e	GRS Odyssey ^f
Na ₂ O	1.3 ± 0.5	1.2	3.3 ± 0.3	2.5	2.9 ± 0.3	2.3 ± 0.5	2.0 ± 0.6	3.8 ± 2.7	—
MgO	11.4 ± 5.8	9.4	9.3 ± 0.2	1.5	12.2 ± 0.5	8.5 ± 0.7	6.2 ± 1.5	7.6 ± 4.0	—
Al ₂ O ₃	7.6 ± 2.7	8.6	10.0 ± 0.2	11.0	11.1 ± 0.5	14.5 ± 2.9	16.7 ± 1.2	12.3 ± 7.0	—
SiO ₂	49.2 ± 1.7	45.7	45.8 ± 0.4	57.0	45.7 ± 0.3	53.9 ± 0.9	58.2 ± 1.0	42.3 ± 10	43 ± 4
K ₂ O	0.12 ± 0.08	0.7	0.41 ± 0.03	1.4	0.06 ± 0.01	0.9 ± 0.5	2.2 ± 0.7	0.45 ± 0.14	0.35 ± 0.1
CaO	9.0 ± 2.0	7.1	6.1 ± 0.3	8.1	7.6 ± 0.1	10.8 ± 0.5	7.5 ± 1.4	9.2 ± 6.0	—
TiO ₂	0.95 ± 0.47	1.1	0.81 ± 0.08	0.69	0.49 ± 0.02	0.18 ± 0.08	0.3 ± 0.3	2.2 ± 1.7	—
Fe ₂ O ₃	20.6 ± 1.7	21.7	17.6* ± 0.4	15.7	19.8* ± 0.3	10.3* ± 4.4	7.7* ± 2.9	12.9 ± 5.2	20 ± 6
U (ppm)	0.1 ± 0.06	—	—	—	—	—	—	0.7 ± 0.2	—
Th (ppm)	0.25 ± 0.27	—	—	—	—	—	—	2.2 ± 0.7	0.7 ± 0.3

GRS, gamma-ray spectrometer; MPF, Mars Pathfinder; MER, Mars Exploration Rover (Spirit); TES, thermal emission spectrometer; sherg., shergottite. Errors where quoted are one standard deviation.

^aMean composition from DaG476/89, Dhofar 019, EETA 79001B, QUE94201, SaU005, Shergotty, Zagami, and Los Angeles.

^bBruckner et al. (2003).

^cMean of compositions in Gellert et al. (2004) (soil) and McSween et al. (2004) (rock).

^dMean of four models in Table 4 of McSween et al. (2003).

^eArea-weighted mean from Surkov et al. (1994).

^fTaylor et al. (2003).

Indicates converted from FeO to Fe₂O₃, which can lead to totals > 100%.

3.12 NIMMO ■ TANAKA

same result: The bulk of the Martian crust was extracted from the mantle sometime around 4.5 Gyr B.P. (Chen & Wasserburg 1986, Borg et al. 1997, Blichert-Toft et al. 1999, Halliday et al. 2001, Nyquist et al. 2001).

Not all basaltic shergottites show the depletion in LREEs expected for a melt generated from an already depleted mantle (Norman 1999, McLennan 2003b). The most likely explanation for this observation is that the basalts incorporated variable amounts of an LREE-enriched component (Longhi 1991, Norman 1999, McLennan 2003b, Nyquist & Shih 2003). A possible analogue for this enriched component is lunar KREEP (McSween et al. 2003), which may comprise roughly half the lunar crust in some areas (Wieczorek & Phillips 2000). Further evidence for assimilation of an enriched component into the basaltic shergottites comes from the correlation between K/Th ratios and K concentrations (McSween et al. 2003), and the correlation between contamination and oxidation state (Wadhwa 2001). This enriched component likely represents the ancient Martian crust.

In situ Martian soil compositions measured by Viking, MPF and the Spirit MER are similar, which suggests a well-mixed global layer, but have less silica and more potassium than basaltic shergottites (Table 1). Both the Spirit MER (McSween et al. 2004) and MPF also measured rock compositions, although for MPF it is not clear that the rocks were igneous (McSween et al. 1999) and the analyses were complicated by calibration problems and the existence of a sulfur-rich surface layer (see Wanke et al. 2001, Bruckner et al. 2003). The rocks measured by Spirit were Mg-rich basalts, probably from a depleted mantle source (McSween et al. 2004). The MPF results implied a soil-free rock (SFR) with an SiO₂ content of 57 wt% (Wanke et al. 2001, Bruckner et al. 2003), which suggests a basaltic andesite or andesitic composition (McSween et al. 2003). Table 1 shows that this SFR has higher concentrations of K and lower Mg concentrations than the mean soil. Wanke et al. (2001) and Bruckner et al. (2003) argued that the soil composition can be generated by a mixture of shergottite and SFR (andesitic) compositions, although mismatches in Si, Fe, and K result (McSween et al. 2003). Overall, the in situ measurements suggest the presence of both basaltic and andesitic end-member components. The Pathfinder SFR may be the best available representative of an andesitic crust on Mars.

Turning to remote sensing, IR observations give mineralogical constraints and GR observations give elemental abundances. Both data sets suffer from the fact that surface compositions may not necessarily be representative of the bulk crustal composition. Furthermore, near-surface Martian materials may have been chemically altered or weathered (Kirkland et al. 2003, McSween et al. 2003, Taylor et al. 2003), which further complicates the interpretation of their chemistry. Nonetheless, existing Odyssey (Taylor et al. 2003) and Phobos-2 (Surkov et al. 1994) GR data give similar compositions to in situ soil analyses (see Table 1).

The IR data can be used only to identify minerals in relatively dust-free areas of the planet and are sensitive only to the top millimeter or so. Initial results argued for the presence of both basaltic (type 1) and andesite-like (type 2) surfaces (Bandfield et al. 2000). This result was particularly intriguing, as the andesite-like material occurred in the northern lowlands. Subsequent work, however, has shown that the

andesite-like signature could also be due to altered basalt (Wyatt & McSween 2002). Analysis of the distribution and geologic context of the type 2 signature suggests that it may result from weathering and eolian redistribution of type 1 material (Wyatt et al. 2004).

On the basis of the inferred mineralogy, various groups have calculated the chemical compositions of the two surface types (Bandfield et al. 2000, Wyatt & McSween 2002, McSween et al. 2003). Despite the different mineralogies assumed, the chemical compositions obtained are rather similar. Furthermore, the calculated compositions of the type 2 surface closely resemble the inferred SFR composition, with the exception of Mg, Fe, and Al (Table 1).

McSween (2002) calculated minimum densities for magmas derived from Martian meteorites of 2800 kg m^{-3} , compared with densities of 2700 kg m^{-3} for magmas derived from the SFR. The inferred density of the SFR itself is 3060 kg m^{-3} (Neumann et al. 2004). The IR-derived mineralogies result in rock densities of $2900\text{--}3000$ and 2700 kg m^{-3} for surface types 1 and 2, respectively. The former (basaltic) density is slightly smaller than the values obtained by admittance studies for young volcanic regions (see Physical Characteristics, above). Magmas derived from Martian meteorites, being lighter, would be capable of erupting through lavas of this density. However, the same lavas would be much less likely to ascend through andesitic rocks with a density of 2700 kg m^{-3} , particularly if their density is reduced by fracture porosity (see Physical Characteristics, above). Potentially, ascending magmas may have been neutrally buoyant in the shallow highland crust, resulting in widespread sill intrusion rather than extrusion.

Geochemical mass balance arguments can be used to place an upper limit on crustal thickness, but they are hampered by uncertainties in both the bulk composition and the crustal composition of Mars. Nonetheless, Norman (1999) used REE abundances in Martian meteorites to derive a crustal thickness of $<45 \text{ km}$. McLennan (2001), Taylor et al. (2003), and Wieczorek & Zuber (2004) used radiogenic element abundances from GR data to infer upper bounds on the crustal thickness of 65 to 93 km .

Summary

Many aspects of the ancient Martian crust are highly uncertain; in particular, although there is strong circumstantial evidence for an enriched crustal component, no meteorite samples of this postulated material exist. Nonetheless, we present a summary of likely crustal characteristics in Table 2. For reasons outlined above, we give two compositions: an andesitic composition representative of the ancient, volumetrically dominant crust, and a basaltic composition representative of later volcanic products.

The densities and thicknesses are based on the admittance observations and mineralogical calculations described above. For the ancient crust, the bulk chemical composition is based on the Pathfinder SFR and TES-derived compositions for surface type 2. An exception is potassium, which is particularly prone to alteration effects (Taylor et al. 2003). Because the Pathfinder soil K concentration exceeds

TABLE 2 Summary of inferred Martian crust compositions, and comparisons with other crustal rocks

Property	Mars type 1	Mars type 2	Earth—bulk cont'l	Earth— oceanic	Lunar highlands	Lunar low-Ti basalts	Lunar KREEP
Mean thickness (km)	—	50	35 ^a	7 ^a	60 ^b	—	Variable (<30) ^c
Mean density (kg m ⁻³)	3100	2700	2750 ^a	3000 ^a	2860 ^b	3300 ^b	3100 ^c
Mean age (Gyr)	3.5	4.5	2.0 ^c	0.06	4.5 ^b	3.2 ^b	3.9 ^b
H (μW m ⁻³)	0.13	0.59	1.34	0.13	0.05	0.28	5.2
Composition	Basalt	Basaltic- andesite	Andesite ^d	Basalt ^d	Anorthosite ^b	Basalt ^b	Basalt ^a
SiO ₂ (wt %)	49.2	57.0	57.3	49.5	45.0	45.7	52.5
Al ₂ O ₃ (wt %)	7.6	11.0	15.9	16.0	25.0	9.3	16.9
K ₂ O (wt %)	0.12	0.7	1.1	0.15	0.075	0.056	0.53
U (ppm)	0.1	0.4	0.9	0.1	0.033	0.19	3.4
Th (ppm)	0.25	1.2	3.5	0.22	0.125	0.71	10.3

H is the crustal heat production rate at 4.1 Gyr B.P. Rationale for Martian crustal properties is discussed in the text.

^aData based on Lodders & Fegley (1998).

^bLunar Sourcebook (Heiken et al. 1991).

^cData based on Taylor & McLennan (1985).

^dData based on Taylor (1992).

^eFrom Wiczorek & Phillips (2000).

the mean GR and MER soil measurements by a factor of 2, we have reduced the inferred crustal K concentration by the same factor. Simple mass balance arguments then show that the GR and MER soil potassium concentrations can be matched by a 50/50 mix of SFR and shergottite end-member compositions (compare with Wanke et al. 2001). With this same mix, the U and Th compositions in the SFR can be deduced from the Phobos-2 GR data. McLennan (2001, 2003a) has arrived at similar numbers. For the recent volcanic crust, the estimates are based mainly on basaltic shergottite measurements, combined with GR and MER observations.

It is likely that, as on the Moon (Taylor 1992), the ancient crust is volumetrically dominant. Norman's (1999) mass balance calculations suggest that at least one third of the total crust is ancient and enriched. Cratering and geological studies (Frey et al. 2002, Head & Kreslavsky 2002, Tanaka et al. 2003b) suggest that the northern plains are filled with hundreds of meters to a few kilometers of material, likely sedimentary and volcanic, and the thickness of probable lava flows at Valles Marineris approaches 10 km (McEwen et al. 1999). Young volcanic edifices such as the Tharsis Montes and Elysium are probably composed predominantly of basaltic material upwards of 10 km in thickness.

The presence of radiogenic elements in the crust can have a significant effect on the crustal temperature structure (McLennan 2001). A hypothetical Noachian temperature profile is plotted in Figure 5, with the crustal radiogenic concentrations given in Table 2. In this model the crust produces 35% of the total planetary radiogenic heat and causes the slight curvature in the crustal temperature profile. The subcrustal heat flux is 41.2 mW m^{-2} , the lithospheric thickness (defined by the 1400 K isotherm) is 73 km, and the effective elastic thickness T_e is 25 km (see figure caption). This latter value is slightly higher than the values obtained above (see Physical Characteristics), probably because it ignores any contribution to the subcrustal heat flux from secular cooling. The crustal temperature profile is compatible with 30 km of magnetized hematite or magnetite, but would not allow pyrrhotite magnetization to this depth.

In summary, the bulk crust is 50 km thick on average and was initially magnetized through most of its depth. The volumetrically dominant, ancient part of the crust was extracted at 4.5 Gyr B.P., is similar to an andesite or basaltic andesite, and is enriched in radiogenic elements, LREEs, and aluminum; it probably resembles the SFR in composition, but it is not represented by any of the Martian meteorites. The second crustal component, produced by subsequent melting of the depleted mantle, is basaltic and probably similar to the shergottites in composition. The soil of Mars is generated by mixing and weathering of these two end-members.

HOW AND WHEN DID IT FORM?

Timing

The main constraint on the timing of crustal formation comes from isotopic systems in Martian meteorites. As discussed above (see Chemical Characteristics), the

3.16 NIMMO ■ TANAKA

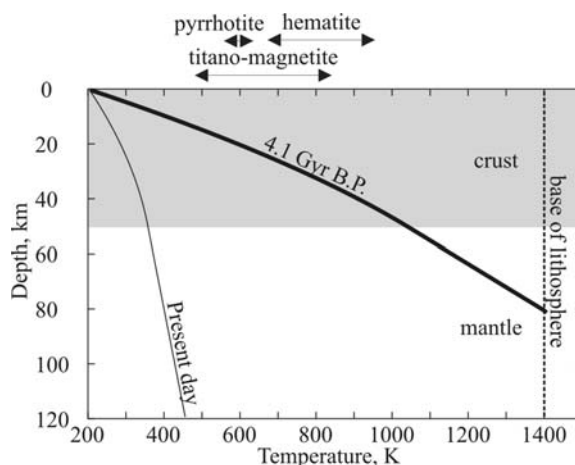


Figure 5 Theoretical temperature profile in Martian crust at 4.1 Gyr B.P. Crustal thickness is 50 km; radiogenic element concentrations are given in Table 2. These elements were extracted from a mantle with initial concentrations given by Wanke & Dreibus (1994). Depleted mantle heat flux is 35.5 mW m^{-2} , surface heat flux is 63.4 mW m^{-2} . Thin line gives present-day temperature profile (mantle and surface heat fluxes of 4.3 and 14.3 mW m^{-2} , respectively). Thermal conductivity is $3 \text{ W m}^{-1} \text{ K}^{-1}$; arrows denote Curie temperatures of likely magnetic minerals. When using the method and parameters of Nimmo & Watters (2004) and a strain rate of 10^{-17} s^{-1} and curvature of $5 \times 10^{-7} \text{ m}^{-1}$, the elastic thickness T_e at 4.1 Gyr B.P. is 25 km.

different systems suggest that the bulk of the Martian crust was extracted at around 4.5 Gyr B.P., that is, within 100 Myr of the planet's formation. This timescale is comparable to or longer than the timescale for Martian core formation, which is about 15 Myr (Kleine et al. 2002). Subsequent additions to the Martian crust, in the form of intrusive and extrusive magmatism, were probably volumetrically minor.

Mode of Formation

The late stage of planetary accretion involves infrequent, very large impacts. The energy of these impacts depends on the overall size of the target body; thus, for Earth-sized targets, global melting is inevitable and a magma ocean results (e.g., Tonks & Melosh 1993). For Mars, it is less clear that a magma ocean is required (Senshu et al. 2002). Siderophile element abundances suggest that the core last equilibrated with the mantle at $\sim 2500 \text{ K}$ and pressures $< 1 \text{ GPa}$, or $< 100 \text{ km}$ depth (Kong et al. 1999). Equilibration within a magma ocean is likely to be rapid, so these results suggest that any such ocean was probably confined to shallow depths. The rapid iron segregation timescale implied by the Hf/W data suggests that either an at least partially molten mantle was present (Stevenson 1990) or that significant mantle deformation was occurring (Bruhn et al. 2000).

Elkins-Tanton et al. (2003) have shown that a deep (>600 km) Martian magma ocean will generate melts depleted in Al (as observed in Martian meteorites) due to sinking of Al-rich garnet. The solidifying magma ocean will ultimately result in a mantle which is chemically stably stratified. This chemical stability may help explain the lack of convective mixing inferred from Martian meteorite isotopic heterogeneity (Halliday et al. 2001). However, it is not yet clear how to reconcile the presence of a deep magma ocean with the siderophile evidence outlined above.

Cooling and crystallization of the initial magma ocean will have been a relatively rapid process (Spohn & Schubert 1991), generating a primordial, cumulate-type crust. Little work to date has been done on the petrological and geophysical implications of such a primordial Martian crust, although subsequent additions to the crust by convection and/or plate tectonics have been modeled by various authors (e.g., Breuer et al. 1993, Hauck & Phillips 2002, Breuer & Spohn 2003). These models generally produce relatively modest melt volumes, which are likely to be basaltic in composition, in agreement with the conclusions of Characteristics of the Ancient Crust, above. More petrological and geophysical investigations of the behavior of Martian magma oceans are required.

Plate Tectonics?

A particularly intriguing hypothesis for crustal formation on Mars is that the northern lowland crust was generated by an episode of sea-floor spreading during the Late Noachian to Early Hesperian (Sleep 1994). Although the original model was motivated by regional geological considerations, there are two theoretical arguments that make plate tectonics attractive. First, plate tectonics is an efficient way of cooling the mantle and thus helps drive an early dynamo (Nimmo & Stevenson 2000). Second, the efficient cooling also provides a way of avoiding early massive melting on Mars (Hauck & Phillips 2002). Unfortunately, the timing of northern plains resurfacing implied by the plate tectonic hypothesis is contradicted by the density of QCDs (Frey 2004) and by the presence of Noachian outcrops and conflicting structural patterns in the northern plains (Pruis & Tanaka 1995). Furthermore, plate tectonics on Earth provides an efficient way of mixing and rehomogenizing at least the upper mantle (e.g., Carlson 1994); the heterogeneous nature of the Martian mantle (Halliday et al. 2001) suggests that no such mixing took place. Nor are the theoretical arguments secure. An initially hot core is an alternative way of driving a Martian dynamo without requiring plate tectonics (Breuer & Spohn 2003, Williams & Nimmo 2004). Although plate tectonics may reduce melting early on, it makes later melt generation, as suggested by observations, more difficult to achieve (Breuer & Spohn 2003).

An alternative is that plate tectonics occurred in the southern highlands. Connerney et al. (1999) argued that the linear magnetic features resembled sea-floor spreading stripes on Earth, and Fairen et al. (2002) suggested that the features were accretionary terrains. Unfortunately, there is little supporting geological or geophysical evidence to bolster these suggestions, so they must be currently regarded as highly speculative.

HOW WAS IT MODIFIED?

Hemispheric Dichotomy

The most striking feature of the present-day Martian crust is that it is significantly thicker in the southern hemisphere than in the northern hemisphere; comparable global-scale thickness contrasts are observed on the Moon (Neumann et al. 1996). This thickness contrast is roughly mirrored by the contrast in surface ages, although there are exceptions. For instance, the crustal thickness beneath Arabia Terra is moderate, but the surface is heavily cratered (Zuber 2001). These two features are collectively called the hemispheric dichotomy. Cratering evidence (Figure 3) suggests that the dichotomy formed at or before 4.12 Gyr B.P., but the origin of the dichotomy is a major unsolved problem in Martian science.

One possibility (the endogenic hypothesis) is that the crust formed with a nonuniform thickness distribution, or developed such a distribution through mantle convection (McGill & Dimitriou 1990). However, the mechanism by which such an initial asymmetry could be produced on Mars is unclear. Zhong & Zuber (2001) suggest that strongly depth-dependent viscosities could result in degree-1 convection that might explain the dichotomy. The southern highlands show signs of contraction (Watters & Robinson 1999, Mueller & Golombek 2004) at their margins, consistent with formation over a hemispheric downwelling. The Zhong & Zuber (2001) hypothesis is attractive because it can explain both the dichotomy and an early dynamo, although whether ~ 100 -fold viscosity variations are likely in the Martian mantle is unclear. One way of generating large vertical viscosity variations is if the Martian mantle is compositionally layered (Kiefer 2003, Jones 2003), perhaps as a result of its original crystallization (Elkins-Tanton et al. 2003), but the geodynamical implications of this model have yet to be explored. We also note that a layered mantle may slow core cooling and thus render dynamo generation more difficult.

The other likely explanation (the exogenic hypothesis) for the hemispheric dichotomy is that the crustal thinning is due to one (Wilhelms & Squyres 1984) or several large impacts that include Utopia and other less well substantiated basins (Frey & Schultz 1988). These impacts must have taken place early in Martian history, since little trace of them exists now. One or a few giant impacts would provide a natural explanation for the near-total demagnetization of the northern lowlands (see Physical Characteristics, above). Subsequent impacts (e.g., Isidis) caused additional demagnetization and modified the topography further. Figure 3 shows a hypothetical timeline for events early in Martian history.

It has been argued that the crustal thickness distribution and dichotomy topography do not support the impact hypothesis (Zuber 2001). However, both the topography and the crustal thickness are likely to have been modified subsequently: the former by erosion, the latter by lower crustal flow, and both by the development of the Tharsis rise (see Tharsis, below) and later impacts. For instance, the gradual transition in crustal thickness across Arabia Terra is likely to be representative of

the original dichotomy; sharper transitions, such as around Isidis, are probably due to modification by impact (Frey 2002). Other signatures of early large impacts, such as thick ejecta blankets, may have been erased by the apparently high rates of erosion during the Noachian (Hynes & Phillips 2001). Accordingly, it is hard to rule out the impact hypothesis on the basis of available observations.

A serious problem with the multiple impact hypothesis is that the generation of the lowlands by several Utopia-scale impacts (Frey & Schultz 1988) has a low probability (McGill & Squyres 1991). Formation of the lowlands by a single, giant (>7000 km) basin cannot be ruled out on statistical grounds (McGill & Squyres 1991). However, it is commonly assumed that impacts capable of generating basins comparable in diameter to the planetary diameter will cause catastrophic disruption of the planet (e.g., Chapman & McKinnon 1986). This assumption needs to be tested with numerical models but, if correct, it makes the single-impact hypothesis untenable.

Although the northern lowlands were undoubtedly significantly modified by impacts, at present we consider it more likely that the lowlands were formed by an endogenic process. Although the time available to develop long-wavelength circulation patterns of the kind required is relatively short, <400 Myr, current models suggest that this timescale is not an insuperable obstacle (e.g., Lenardic et al. 2004b, Roberts & Zhong 2004a). Future challenges will involve coupling the mantle circulation to the deformable crust and explaining the almost complete absence of observable magnetic anomalies in the lowlands.

Tharsis

After the hemispheric dichotomy, the most obvious topographic feature on the Martian surface is the Tharsis rise (Figure 4). The rise consists of a broad (~5000 km) topographic uplift, with several large (~25 km high) volcanoes superimposed on it. Some of the volcanoes have lava flows dated at <40 Ma (Hartmann et al. 1999). The measured elastic thicknesses at the Tharsis volcanoes are generally larger than typical Noachian values (McKenzie et al. 2002, McGovern et al. 2004) and indicate that substantial volcanic construction occurred after lithospheric rigidity had increased (see Physical Characteristics, above).

However, there are several arguments that suggest that the bulk of Tharsis was formed by the Late Noachian (Phillips et al. 2001). First, the orientation of Noachian tectonic features, mainly S and E of the center of Tharsis (Anderson et al. 2001), is consistent with models of the elastic stresses generated by the present-day Tharsis topography (Banerdt & Golombek 2000). Second, the orientation of Noachian-age valley network systems appears to have been influenced by Tharsis loading (Phillips et al. 2001). Third, the existence of magnetic anomalies in the elevated southern flanks of the Tharsis rise suggests that some volcanic construction was occurring while the dynamo was still active (Johnson & Phillips 2004). And finally, the identification of layered deposits in Valles Marineris as flood basalts of Noachian age (McEwen et al. 1999) strongly suggests an active Tharsis source.

These observations collectively imply that Tharsis is predominantly an ancient, albeit long-lived, feature.

The formation of Tharsis had global consequences. For instance, much of the long-wavelength gravity, in particular the low surrounding Tharsis (Figure 4), is a consequence of the loading event (Phillips et al. 2001). The early volcanic outgassing accompanying the development of Tharsis may have had a significant effect on the Martian climate (Phillips et al. 2001). Finally, the development of Tharsis will have had a major influence on the moment of inertia of the planet, quite possibly leading to axial reorientation (Willemann 1984). There have been suggestions based on isolated magnetic anomalies that such polar wander has occurred (Arkani-Hamed 2001, Hood & Zakharian 2001), but the poor spatial resolution of the magnetic data leads to large uncertainties in the claimed amounts of polar wander, and expected tectonic features caused by polar wander have not been found (Grimm & Solomon 1986).

It is unclear what fraction of the present-day Tharsis rise is supported by crustal buoyancy or flexure (Phillips et al. 2001, Zhong 2002), and what fraction is supported by convective stresses (e.g., Harder & Christensen 1996, Kiefer 2003). Because both the load and the lithospheric rigidity have varied with time, the resulting signature is complicated, but the former effect is thought to be dominant (Roberts & Zhong 2004b). Some component of upwelling must be present to explain the recent generation of lavas (Kiefer 2003), and it is likely that this upwelling has persisted for the entire history of Tharsis. Both the size and the inferred stability of the upwelling are unusual in convective systems and may be due to a deep phase transition (Harder & Christensen 1996), variable mantle thermal conductivity (Schott et al. 2001), or chemical layering (Wenzel et al. 2004).

If the bulk of Tharsis was in place by the Late Noachian, then the estimated local elastic thicknesses of ~ 100 km (Phillips et al. 2001, Roberts & Zhong 2004b) are in sharp contrast to the values of < 16 km obtained for the southern highlands (see Physical Characteristics, above). Taken at face value, these results suggest either significant lateral T_e variations or (more likely) a reduction in surface heat flux by a factor > 6 over a period of ~ 600 Myr. Because the convective heat flux scales as viscosity^{-1/3} (e.g., Nimmo & Stevenson 2000) this heat flux reduction implies that the mantle viscosity increased by a factor of ~ 200 . For an activation energy of ~ 500 kJ mol⁻¹ (Karato & Wu 1993), such a viscosity increase requires a mantle temperature drop of ~ 300 K. This high mantle cooling rate requires very high initial mantle temperatures, and probably a large component of heat transport by melt generation and/or extraction of radiogenic elements (e.g., Reese et al. 1998). The high cooling rate also favors the generation of an early Martian dynamo (Nimmo & Stevenson 2000).

Subsequent (Noachian) Modification

Once the crustal dichotomy was in place, it is likely to have modified mantle convection behavior. Breuer et al. (1993) and Wullner & Harder (1998) showed

that latitudinal variations in crustal heat production were likely to lead to different mantle behavior in the two hemispheres. Lateral variations in lithospheric temperature structure can also result in upwellings localized at the boundary (King & Ritsema 2000). Lenardic et al. (2004a) argued that the growth of a buoyant crustal layer could shut off plate tectonics once the layer exceeded a critical fraction of the total surface area. Wenzel et al. (2004) found that upwellings were focused in the southern highlands, and showed that for a layered mantle the resulting upwellings were stable over the age of Mars. Thus, it is quite likely that the development of the dichotomy had a major role in the development of the Tharsis rise.

The dichotomy also appears to have been heavily modified since its formation. For instance, the Isidis and perhaps the Utopia impacts altered the expression of the dichotomy in the eastern hemisphere (Frey 2002). The surface expression of the dichotomy, and the Noachian crust in general, was significantly degraded in places (Craddock & Maxwell 1993; Hynek & Phillips 2001, 2003), probably because of more clement climatic conditions (Craddock & Howard 2002). Later impacts, as noted above (see Physical Characteristics, above), apparently demagnetized the crust. The large impact basins were filled to a greater or lesser extent with sediments and/or lavas. Some of the basins (e.g., Utopia and Isidis) show positive gravity anomalies, indicating a substantial lithospheric rigidity ($T_e \sim 100$ km) at the time the loads were emplaced (Comer et al. 1985, Zuber et al. 2000).

Tectonic modification of the crust during the Noachian appears to have been relatively subdued. Extensional grabens, possibly underlain by dikes (McKenzie & Nimmo 1999), were emplaced south and east of the Tharsis rise and near Alba Patera and Tempe Terra (Anderson et al. 2001). The Tharsis area also saw the development of contractional wrinkle ridges and buckling features during the Late Noachian (Schultz & Tanaka 1994, Mueller & Golombek 2004). The eastern half of the dichotomy experienced lithospheric extension and/or collapse of scarp-forming material along the boundary, and contraction a few hundred kilometers south of the boundary, during the Late Noachian to Early Hesperian (Schultz 2003, Tanaka et al. 2003b, Watters 2003). Strain rates during the Noachian are poorly constrained, although Wilkins et al. (2002) estimate a strain rate of 10^{-11} to 10^{-12} years⁻¹ for the Tempe Terra region, similar to intracontinental regions on Earth.

SUMMARY

The Martian crust probably consists of two main types (Table 2). The volumetrically dominant type is likely rich in silica, aluminum, and heat-producing elements, formed at 4.5 Ga, possibly by crystallization from a magma ocean, and has a relatively low density. It is not represented by any Martian meteorite; its composition is inferred from that of the Pathfinder soil-free rock and remote-sensing observations. The other crustal type is a dense basalt, is relatively well represented in the meteorite record, and consists of younger, areally extensive lava flows overlying the andesitic or basaltic-andesite basement.

3.22 NIMMO ■ TANAKA

The bulk crust is about 50 km thick on average and is magnetized in places to a significant fraction of this depth. The lithospheric rigidity during the early Noachian was low ($T_e \sim 15$ km), consistent with models of the Noachian geothermal profile (Figure 5), but was higher ($T_e \sim 100$ km) by the end of this period, suggesting rapid mantle cooling. The hemispheric dichotomy was probably formed by early long-wavelength mantle convection, although it was subsequently heavily modified by large impacts. Construction of the Tharsis rise, accompanied by local tectonism, probably began shortly after the establishment of the dichotomy, and may indeed have been influenced by it. Early in the development of Tharsis, the magnetic field failed.

Some parts of the summary outlined above are speculative. In particular, three outstanding questions remain. First, although the circumstantial evidence for an andesite-like crustal component is relatively strong, its existence will remain somewhat hypothetical until either an appropriate Martian meteorite is discovered or more convincing in situ measurements are made. With the current MERs, and planned 2009 Mars Science Laboratory, the latter eventuality at least may be realized.

Second, the nature of the magnetic anomalies on Mars, and what they are telling us about the planet's history, remains poorly understood. This is mainly because of the poor spatial resolution of the data; measurements taken at lower altitudes should help resolve some of the issues, especially the magnetization depth. The nature of the mineral phase responsible for the magnetization is likely to be resolved only by in situ analysis.

Finally, the hemispheric dichotomy still remains mysterious, nearly thirty years after its identification. Here we have favored an endogenic explanation (convection), but we do not regard the issue as closed. The identification of an ancient basement beneath the northern plains is a particularly important constraint on the dichotomy's origin, as is the general absence of observable magnetic anomalies in the lowlands. Both further mapping and better numerical models are required to resolve this long-standing issue.

ACKNOWLEDGMENTS

We are grateful for the comments of Pat McGovern, Jim Skinner, Alan Treiman, Pierre Williams and an anonymous reviewer. This work supported by NASA-MDAP NAG5-10587.

**The *Annual Review of Earth and Planetary Science* is online at
<http://earth.annualreviews.org>**

LITERATURE CITED

- | | |
|---------------------------------------------------------------------------------------------------------------------------------------|--------------------------------------------------------------|
| Acuna MH, Connerney JE, Ness NF, Lin RP, Mitchell D, et al. 1999. Global distribution of crustal magnetization discovered by the Mars | Global Surveyor MAG/ER experiment. <i>Science</i> 284:790–93 |
| | Albee AL, Arvidson RE, Palluconi F, Thorpe T. |

2001. Overview of the Mars Global Surveyor mission. *J. Geophys. Res.* 106:23291–316
- Anderson RC, Dohm JM, Golombek MP, Haldemann AFC, Franklin BJ, et al. 2001. Primary centers and secondary concentrations of tectonic activity through time in the western hemisphere of Mars. *J. Geophys. Res.* 106:20563–85
- Antretter M, Fuller M, Scott E, Jackson M, Moskowitz B, Solheid P. 2003. Paleomagnetic record of Martian meteorite ALH84001. *J. Geophys. Res.* 108:5049
- Arkani-Hamed J. 2001. Paleomagnetic pole positions and pole reversals of Mars. *Geophys. Res. Lett.* 28:3409–12
- Arkani-Hamed J. 2002. An improved 50-degree spherical harmonic model of the magnetic field of Mars derived from both high-altitude and low-altitude data. *J. Geophys. Res.* 107: 5083
- Banerdt WB, Golombek MP. 2000. Tectonics of the Tharsis region of Mars: insights from MGS topography and gravity. *Lunar Planet Sci. Conf. XXXI*. Abstr. 2038
- Bandfield JL, Hamilton VE, Christensen PR. 2000. A global view of Martian surface compositions from MGS-TES. *Science* 287: 1626–30
- Blichert-Toft J, Gleason JD, Telouk P, Albarede F. 1999. The Lu-Hf isotope geochemistry of shergottites and the evolution of the Martian mantle-crust system. *Earth Planet. Sci. Lett.* 173:25–39
- Borg LE, Nyquist LE, Taylor LA, Wiesmann H, Shih C-Y. 1997. Constraints on Martian differentiation processes from Rb-Sr and Sm-Nd isotopic analyses of the basaltic shergottite QUE94201. *Geochim. Cosmochim. Acta* 61:4915–31
- Breuer D, Spohn T. 2003. Early plate tectonics versus single-plate tectonics on Mars: evidence from magnetic field history and crust evolution. *J. Geophys. Res.* 108:5072
- Breuer D, Spohn T, Wullner U. 1993. Mantle differentiation and the crustal dichotomy of Mars. *Planet. Space Sci.* 41:269–83
- Bruckner J, Dreibus G, Rieder R, Wanke H. 2003. Refined data of Alpha Proton X-ray spectrometer analyses of soils and rocks at the Mars Pathfinder site: implications for surface chemistry. *J. Geophys. Res.* 108:8094
- Bruhn D, Groebner N, Kohlstedt DL. 2000. An interconnected network of core-forming melts produced by shear deformation. *Nature* 403:883–86
- Cain JC, Ferguson BB, Mozzoni D. 2003. An $n = 90$ internal potential function of the Martian crustal magnetic field. *J. Geophys. Res.* 108:5008
- Carlson RW. 1994. Mechanisms of Earth differentiation: consequences for the chemical structure of the mantle. *Rev. Geophys.* 32: 337–61
- Carr MH. 1979. Formation of Martian flood features by release of water from confined aquifers. *J. Geophys. Res.* 84:2995–3007
- Chapman CR, McKinnon WB. 1986. Cratering of planetary satellites. In *Satellites*, Burns JA, Matthews MS, eds. Tucson: Univ. Ariz. Press
- Chen JH, Wasserburg GJ. 1986. Formation ages and evolution of Shergotty and its parent planet from U-Th-Pb systematics. *Geochim. Cosmochim. Acta* 50:955–68
- Clifford SM. 1993. A model for the hydrologic and climatic behavior of water on Mars. *J. Geophys. Res.* 98:10973–1016
- Clifford SM, Parker TJ. 2001. The evolution of the Martian hydrosphere: implications for the fate of a primordial ocean and the current state of the northern plains. *Icarus* 154:40–79
- Comer RP, Solomon SC, Head JW. 1985. Mars: thickness of the lithosphere from the tectonic response to volcanic loads. *Rev. Geophys.* 23: 61–92
- Connerney JEP, Acuna MH, Wasilewski PJ, Kletetschka G, Ness NF, et al. 2001. The global magnetic field of Mars and implications for crustal evolution. *Geophys. Res. Lett.* 28:4015–18
- Connerney JEP, Acuna MH, Wasilewski P, Ness NF, Reme H, et al. 1999. Magnetic lineations in the ancient crust of Mars. *Science* 284:794–98
- Craddock RA, Howard AD. 2002. The case for rainfall on a warm, wet early Mars. *J. Geophys. Res.* 107:5111

3.24 NIMMO ■ TANAKA

- Craddock RA, Maxwell TA. 1993. Geomorphic evolution of the Martian highlands through ancient fluvial processes. *J. Geophys. Res.* 98:3453–68
- Dohm JM, Tanaka KL, Hare TM. 2001. Geologic, paleotectonic and paleoerosional maps of the Thaumasia region, Mars. *U.S. Geol. Surv. Misc. Invest. Ser. Map I-2650*
- Elkins-Tanton LT, Parmentier EM, Hess PC. 2003. Magma ocean fractional crystallization and cumulate overturn in terrestrial planets: implications for Mars. *Meteor. Planet. Sci.* 38:1753–71
- Fairen AG, Ruiz J, Anguita F. 2002. An origin for the linear magnetic anomalies on Mars through accretion of terranes: implications for dynamo timing. *Icarus* 160:220–23
- Frey H, Schultz RA. 1988. Large impact basins and the mega-impact origin for the crustal dichotomy on Mars. *Geophys. Res. Lett.* 15:229–32
- Frey HV. 2002. Age and origin of the crustal dichotomy in Eastern Mars. *Lunar Planet. Sci. Conf. XXXIII*. Abstr. 1727
- Frey HV. 2004. A timescale for major events in early Mars crustal evolution. *Lunar Planet. Sci. Conf. XXXV*. Abstr. 1382
- Frey HV, Roark JH, Shockey KM, Frey EL, Sakimoto SHE. 2002. Ancient lowlands on Mars. *Geophys. Res. Lett.* 29:1384
- Gellert R, Rieder R, Anderson RC, Bruckner J, Clark BC, et al. 2004. Chemistry of rocks and soils in Gusev crater from the Alpha particle X-ray spectrometer. *Science* 305:829–32
- Golombek MP, Cook RA, Economou T, Folkner WM, Haldemann AFC, et al. 1997. Overview of the Mars Pathfinder mission and assessment of landing site predictions. *Science* 278:1743–48
- Greeley R, Spudis P. 1981. Volcanism on Mars. *Rev. Geophys.* 19:13–41
- Grimm RE, Solomon SC. 1986. Tectonic tests of proposed polar wander paths for Mars and the Moon. *Icarus* 65:110–21
- Halliday AN, Wanke H, Birk J-L, Clayton RN. 2001. The accretion, composition and early differentiation of Mars. *Space Sci. Rev.* 96:197–230
- Harder H, Christensen UR. 1996. A one-plume model of Martian mantle convection. *Nature* 380:507–9
- Harrison KP, Grimm RE. 2002. Controls on Martian hydrothermal systems: application to valley networks and magnetic anomaly formation. *J. Geophys. Res.* 107:5025
- Hartmann WK. 1978. Martian cratering. V. Toward an empirical Martian chronology, and its implications. *Geophys. Res. Lett.* 5:450–52
- Hartmann WK, Malin M, McEwen A, Carr M, Soderblom L, et al. 1999. Evidence for recent volcanism on Mars from crater counts. *Nature* 397:586–89
- Hartmann WK, Neukum G. 2001. Cratering chronology and the evolution of Mars. *Space Sci. Rev.* 96:165–94
- Hauck SA, Phillips RJ. 2002. Thermal and crustal evolution of Mars. *J. Geophys. Res.* 107:5052
- Head JW, Kreslavsky MA. 2002. Northern lowlands of Mars: evidence for widespread volcanic flooding and tectonic deformation in the Hesperian period. *J. Geophys. Res.* 107:5003
- Heiken G, Vaniman D, French BM. 1991. *Lunar Sourcebook: A User's Guide to the Moon*. New York: Cambridge Univ. Press. 736 pp.
- Hess PC. 1989. *Origins of Igneous Rocks*. Cambridge, MA: Harvard Univ. Press
- Hood LL, Zakharian A. 2001. Mapping and modeling of magnetic anomalies in the northern polar regions of Mars. *J. Geophys. Res.* 106:14601–19
- Hood LL, Richmond NC, Pierazzo E, Rochette P. 2003. Distribution of crustal magnetic fields on Mars: shock effects of basin-forming impacts. *Geophys. Res. Lett.* 30:1281
- Hynek BM, Phillips RJ. 2001. Evidence for extensive denudation of the Martian highlands. *Geology* 29:407–10
- Hynek BM, Phillips RJ. 2003. New data reveal mature, integrated drainage systems on Mars indicative of past precipitation. *Geology* 31:757–60
- Irwin RP, Howard AD. 2002. Drainage basin

- p>evolution in Noachian Terra Cimmeria, Mars.
- J. Geophys. Res.*
- 107:5056
- Irwin RP, Maxwell TA, Howard AD, Craddock RA, Leverington DW. 2002. A large paleolake basin at the head of Ma'adim Vallis, Mars. *Science* 296:2209–12
- Ivanov BA. 2001. Mars/Moon cratering rate ratio estimates. *Space Sci. Rev.* 96:87–104
- Johnson CL, Phillips RJ. 2004. Evolution of the Tharsis region of Mars: insights from magnetic field observations. *Earth Planet. Sci. Lett.* In press
- Johnson HP, Salem BL. 1994. Magnetic properties of dikes from the oceanic upper crustal section. *J. Geophys. Res.* 99:21733–40
- Jones JH. 2003. Constraints on the structure of the Martian interior determined from the chemical and isotopic systematics of SNC meteorites. *Meteor. Planet. Sci.* 38:1807–14
- Kallenbach R, Geiss J, Hartmann WK, eds. 2001. *Chronology and Evolution of Mars*. Dordrecht: Kluwer
- Karato S, Wu P. 1993. Rheology of the upper mantle: a synthesis. *Science* 260:771–78
- Kiefer WS. 2003. Melting in the Martian mantle: shergottite formation and implications for present-day mantle convection on Mars. *Meteor. Planet. Sci.* 38:1815–32
- Kieffer HH, Jakosky BM, Snyder CW, Matthews MS, eds. 1992. *Mars*. Tucson: Univ. Ariz. Press
- King SD, Ritsema J. 2000. African hot spot volcanism: small-scale convection in the upper mantle beneath cratons. *Science* 290:1137–40
- Kirkland LE, Herr KC, Adams PM. 2003. Infrared stealthy surfaces: why TES and THEMIS may miss some substantial mineral deposits on Mars and implications for remote sensing of planetary surfaces. *J. Geophys. Res.* 108:5137
- Kleine T, Munker C, Mezger K, Palme H. 2002. Rapid accretion and early core formation on asteroids and terrestrial planets from Hf-W chronometry. *Nature* 418:952–55
- Kletetschka G, Wasilewski PJ, Taylor PT. 2000. Mineralogy of the sources for magnetic anomalies on Mars. *Meteor. Planet. Sci.* 35:895–99
- Kong P, Ebihara M, Palme H. 1999. Siderophile elements in Martian meteorites and implications for core formation in Mars. *Geochim. Cosmochim. Acta* 63:1865–75
- Kristjansson L, Johannesson H. 1999. Secular variations and reversals in a composite 2.5 km thick lava section in central Western Iceland. *Earth Planets Space* 51:261–76
- Lenardic A, Nimmo F, Moresi L. 2004a. Growth of the hemispheric dichotomy and the cessation of plate tectonics on Mars. *J. Geophys. Res.* 109:E02003
- Lenardic A, Richards MA, Busse FH, Morris SJS. 2004b. Depth-dependent rheology and the wavelength of mantle convection with application to Mars. *Workshop on Hemispheres Apart*, pp. 39–40. Lunar Planet. Inst., Houston, TX.
- Lodders K. 1998. A survey of shergottite, nakhlite and chassigny meteorites whole-rock compositions. *Meteor. Planet. Sci.* 33: A183–90
- Lodders K, Fegley B. 1998. *The Planetary Scientist's Companion*. Oxford, UK: Oxford Univ. Press. 400 pp.
- Longhi J. 1991. Complex magmatic processes on Mars: inferences from the SNC meteorites. *Proc. Lunar Planet. Sci.* 21:695–709
- MacKinnon DJ, Tanaka KL. 1989. The impacted Martian crust: structure, hydrology, and some geologic implications. *J. Geophys. Res.* 94:17359–70
- Malin MC, Edgett KS. 2000. Sedimentary rocks of early Mars. *Science* 290:1927–37
- McEwen AS, Malin MC, Carr MH, Hartmann WK. 1999. Voluminous volcanism on early Mars revealed in Valles Marineris. *Nature* 397:584–86
- McGill GE, Dimitriou AM. 1990. Origin of the Martian global dichotomy by crustal thinning in the Late Noachian or early Hesperian. *J. Geophys. Res.* 95:12595–605
- McGill GE, Squyres SW. 1991. Origin of the Martian crustal dichotomy: evaluating the hypotheses. *Icarus* 93:386–93
- McGovern PJ, Solomon SC, Smith DE,

3.26 NIMMO ■ TANAKA

- Zuber MT, Simons M, et al. 2002. Localized gravity/topography admittance and correlation spectra on Mars: implications for regional and global evolution. *J. Geophys. Res.* 107:5136
- McGovern PJ, Solomon SC, Smith DE, Zuber MT, Simons M, et al. 2004. Correction to "Localized gravity/topography admittance and correlation spectra on Mars: implications for regional and global evolution." *J. Geophys. Res.* 109:E07007
- McKenzie D, Barnett DN, Yuan DN. 2002. The relationship between Martian gravity and topography. *Earth Planet. Sci. Lett.* 195:1–16
- McKenzie D, Nimmo F. 1999. The generation of Martian floods by the melting of ground ice above dykes. *Nature* 397:231–33
- McLennan SM. 2001. Crustal heat production and the thermal evolution of Mars. *Geophys. Res. Lett.* 28:4019–22
- McLennan SM. 2003a. Composition and chemical evolution of the Martian crust and mantle: integrating the data from missions and meteorites. *Sixth Int. Conf. Mars*. Abstr. 3099
- McLennan SM. 2003b. Large-ion lithophile element fractionation during the early differentiation of Mars and the composition of the Martian primitive mantle. *Meteor. Planet. Sci.* 38:1–12
- McSween HY. 1994. What we have learned about Mars from SNC meteorites. *Meteor. Planet. Sci.* 29:757–79
- McSween HY, Arvidson RE, Bell JF, Blaney D, Cabrol NA, et al. 2004. Basaltic rocks analyzed by the Spirit Rover in Gusev crater. *Science* 305:842–45
- McSween HY. 2002. The rocks of Mars, from far and near. *Meteor. Planet. Sci.* 37:7–25
- McSween HY, Grove TL, Wyatt MB. 2003. Constraints on the composition and petrogenesis of the Martian crust. *J. Geophys. Res.* 108:5135
- McSween HY, Murchie SL, Crisp JA, Bridges NT, Anderson RC, et al. 1999. Chemical, multispectral, and textural constraints on the composition and origin of rocks at the Mars Pathfinder landing site. *J. Geophys. Res.* 104:8679–715
- Mitchell DL, Lin RP, Mazelle C, Reme H, Cloutier PA, et al. 2001. Probing Mars' crustal magnetic field and ionosphere with the MGS Electron Reflectometer. *J. Geophys. Res.* 106:23419–27
- Mohit PS, Arkani-Hamed J. 2004. Impact demagnetization of the Martian crust. *Icarus* 168:305–17
- Moore HJ. 2001. Geologic map of the MTM 40092, 40087, 35092, 35087, and 35082 quadrangles, Tempe-Mareotis region of Mars. *U.S. Geol. Surv. Misc. Invest. Ser. Map I-2727*
- Moore JM, Wilhelms DE. 2001. Hellas as a possible site of ancient ice-covered lakes on Mars. *Icarus* 154:258–76
- Mueller K, Golombek M. 2004. Compressional structures on Mars. *Annu. Rev. Earth Planet. Sci.* 32:435–64
- Neumann GA, Zuber MT, Smith DE, Lemoine FG. 1996. The lunar crust: global structure and signature of major basins. *J. Geophys. Res.* 101:16841–63
- Neumann GA, Zuber MT, Wieczorek MA, McGovern PJ, Lemoine FG, Smith DE. 2004. The crustal structure of Mars from gravity and topography. *J. Geophys. Res.* 109:E08002
- Nimmo F. 2000. Dike intrusion as a possible cause of linear Martian magnetic anomalies. *Geology* 28:391–94
- Nimmo F. 2002. Admittance estimates of mean crustal thickness and density at the Martian hemispheric dichotomy. *J. Geophys. Res.* 107:5117
- Nimmo F, Gilmore MS. 2001. Constraints on the depth of magnetized crust on Mars from impact craters. *J. Geophys. Res.* 106:12315–23
- Nimmo F, Stevenson D. 2000. The influence of plate tectonics on the thermal evolution and magnetic field of Mars. *J. Geophys. Res.* 105:11969–80
- Nimmo F, Stevenson D. 2001. Estimates of Martian crustal thickness from viscous relaxation of topography. *J. Geophys. Res.* 106:5085–98
- Nimmo F, Watters TR. 2004. Depth of faulting

- on Mercury: implications for heat flux and crustal and effective elastic thickness. *Geophys. Res. Lett.* 31:L02701
- Norman MD. 1999. The composition and thickness of the Martian crust estimated from rare earth elements and neodymium-isotopic composition of Martian meteorites. *Meteor. Planet. Sci.* 34:439–49
- Nyquist LE, Bogard DD, Shih C-Y, Greshake A, Stoffer D, Eugster O. 2001. Ages and geologic histories of Martian meteorites. *Space Sci. Rev.* 98:105–64
- Nyquist LE, Shih C-Y. 2003. Searching for the crustal component in Martian meteorites. *Goldschmidt Conf. Abstr.* A343
- Pariso JE, Johnson HP. 1991. Alteration processes at Deep Sea Drilling Project/Ocean Drilling Program Hole 504B at the Costa Rica rift: implications for magnetization of oceanic crust. *J. Geophys. Res.* 96:11703–22
- Pariso JE, Johnson HP. 1993. Do layer 3 rocks make a significant contribution to marine magnetic anomalies? In situ magnetization of gabbros at Ocean Drilling Program Hole 735B. *J. Geophys. Res.* 98:16033–52
- Parker TJ, Saunders RS, and Schneeberger DM. 1989. Transitional morphology in west Deuteronilus Mensae, Mars: implications for modification of the lowland/upland boundary. *Icarus* 82:111–45
- Phillips RJ, Zuber MT, Solomon SC, Golombek MP, Jakosky BM, et al. 2001. Ancient geodynamics and global-scale hydrology on Mars. *Science* 291:2587–91
- Pruis MJ, Tanaka KL. 1995. The Martian northern plains did not result from plate tectonics. *Lunar Planet. Sci. Conf. XXVI. Abstr.* 1147–48
- Purucker M, Ravat D, Frey H, Voorhies C, Sabaka T, Acuna M. 2000. An altitude-normalized magnetic map of Mars and its interpretation. *Geophys. Res. Lett.* 27:2449–52
- Reese CC, Solomatov VS, Moresi LN. 1998. Heat transport efficiency for stagnant lid convection with dislocation viscosity: Application to Mars and Venus. *J. Geophys. Res.* 103:13643–57
- Roberts JH, Zhong SJ. 2004a. Degree-1 mantle convection as a process for generating the Martian hemispheric dichotomy. *Workshop on Hemispheres Apart*, pp. 52–53. Lunar Planet. Inst., Houston, TX.
- Roberts JH, Zhong SJ. 2004b. Plume-induced topography and geoid anomalies and their implications for the Tharsis rise on Mars. *J. Geophys. Res.* 109:E03009
- Rochette P, Fillion G, Ballou R, Brunet F, Ouladdiaf B, Hood L. 2003. High pressure magnetic transition in pyrrhotite and impact demagnetization on Mars. *Geophys. Res. Lett.* 30:1683
- Rochette P, Lorand JP, Fillion G, Sautter V. 2001. Pyrrhotite and the remanent magnetization of SNC meteorites: a changing perspective on Martian magnetism. *Earth Planet. Sci. Lett.* 190:1–12
- Saunders RS, Arvidson R, Badhwar G, Boynton W, Christensen P, et al. 2004. 2001 Mars Odyssey mission summary. *Space Sci. Rev.* 110:1–36
- Schott B, van den Berg AP, Yuen DA. 2001. Focused time-dependent Martian volcanism from chemical differentiation coupled with variable thermal conductivity. *Geophys. Res. Lett.* 28:4271–74
- Schubert G, Russell CT, Moore WB. 2000. Timing of the Martian geodynamo. *Nature* 408:666–67
- Schultz PH, Schultz RA, Rogers J. 1982. Structure and evolution of ancient impact basins on Mars. *J. Geophys. Res.* 87:9803–20
- Schultz RA. 2003. Seismotectonics of the Amenthes Rupes thrust fault populations, Mars. *Geophys. Res. Lett.* 30:1303
- Schultz RA, Tanaka KL. 1994. Lithospheric-scale buckling and thrust structures on Mars: the Coprates rise and South Tharsis ridge belt. *J. Geophys. Res.* 99:8371–85
- Scott DH, Carr MH. 1978. Geologic map of Mars. *U.S. Geol. Surv. Misc. Invest. Ser. Map I-1083*
- Scott DH, Tanaka KL, Greeley R, Guest JE. 1986–1987. Geologic maps of the western and eastern equatorial and polar regions of

3.28 NIMMO ■ TANAKA

- Mars. *U.S. Geol. Surv. Misc. Invest. Ser. Map11802-A, B, C*
- Senshu H, Kuramoto K, Matsui T. 2002. Thermal evolution of a growing Mars. *J. Geophys. Res.* 107:5118
- Sleep NH. 1994. Martian plate tectonics. *J. Geophys. Res.* 99:5639–55
- Spohn T, Acuna MH, Breuer D, Golombek M, Greeley R, et al. 2001. Geophysical constraints on the evolution of Mars. *Space Sci. Rev.* 96:231–62
- Spohn T, Schubert G. 1991. Thermal equilibration of the Earth following a giant impact. *Geophys. J. Int.* 107:163–70
- Squyres SW, Arvidson RE, Bell JF, Bruckner J, Cabrol NA, et al. 2004. The Spirit Rover's Athena science investigation at Gusev Crater, Mars. *Science* 305:794–99
- Stevenson DJ. 1990. Fluid dynamics of core formation in Newson HE. In *Origin of the Earth*, ed. JH Jones, pp. 231–49. Oxford, UK: Oxford Univ. Press
- Surkov YA, Moskaleva LP, Zolotov MY, Kharynkova VP, Manvelyan OS, et al. 1994. Phobos-2 data on Martian surface geochemistry. *Geochem. Int.* 31:50–58
- Tanaka KL. 1986. The stratigraphy of Mars. *J. Geophys. Res.* 91:E139–58
- Tanaka KL. 2000. Dust and ice deposition in the Martian geologic record. *Icarus* 144:254–66
- Tanaka KL, Banerdt WB, Kargel JS, Hoffman N. 2001. Huge, CO₂-charged debris-flow deposit and tectonic sagging in the northern plains of Mars. *Geology* 27:427–30
- Tanaka KL, Carr MH, Skinner JA, Gilmore MS, Hare TM. 2003a. Geology of the MER 2003 "Elysium" candidate landing site in southeastern Utopia Planitia, Mars. *J. Geophys. Res.* 108:8079
- Tanaka KL, Golombek MP, Banerdt WB. 1991. Reconciliation of stress and structural histories of the Tharsis region of Mars. *J. Geophys. Res.* 95:15617–33
- Tanaka KL, Isbell NK, Scott DH, Greeley R, Guest JE. 1988. The resurfacing history of Mars: a synthesis of digitized, Viking-based geology. *Proc. Lunar Planet. Sci. XVIII*, pp. 665–78
- Tanaka KL, Scott DH, Greeley R. 1992. Global stratigraphy. See Kieffer et al. 1992, pp. 345–82
- Tanaka KL, Skinner JA, Hare TM, Joyal T, Wenker A. 2003b. Resurfacing history of the northern plains of Mars based on geologic mapping of Mars Global Surveyor data. *J. Geophys. Res.* 108:8043
- Taylor GJ, Boynton W, Hamara D, Kerry K, Janes D, et al. 2003. Igneous and aqueous processes on Mars: evidence from measurements of K and Th by the Mars Odyssey gamma ray spectrometer. *Sixth. Int. Conf. Mars*. Abstr. 3207
- Taylor SR. 1992. *Solar System Evolution*. Cambridge, UK: Cambridge Univ. Press
- Taylor SR, McLennan SM. 1985. *The Continental Crust: Its Composition and Evolution*. Oxford, UK: Blackwell
- Tonks WB, Melosh HJ. 1993. Magma ocean formation due to giant impacts. *J. Geophys. Res.* 98:5319–33
- Turcotte DL, Shcherbakov R, Malamud BD, Kucinskas AB. 2002. Is the Martian crust also the Martian elastic lithosphere? *J. Geophys. Res.* 107:5091
- Voorhies CV, Sabaka TJ, Purucker M. 2002. On magnetic spectra of Earth and Mars. *J. Geophys. Res.* 107:5034
- Wadhwa M. 2001. Redox state of Mars' upper mantle and crust from Eu anomalies in shergottite pyroxenes. *Science* 291:1527–30
- Wanke H, Bruckner J, Dreibus G, Rieder R, Ryabchikov I. 2001. Chemical composition of rocks and soils at the Pathfinder site. *Space Sci. Rev.* 96:317–30
- Wanke H, Dreibus G. 1994. Chemistry and accretion history of Mars. *Philos. Trans. R. Soc. London A* 349:285–93
- Watters TR. 1993. Compressional tectonism on Mars. *J. Geophys. Res.* 98:17049–60
- Watters TR. 2003. Thrust faults along the dichotomy boundary in the eastern hemisphere of Mars. *J. Geophys. Res.* 108:5054
- Watters TR, Robinson MS. 1999. Lobate scarps and the Martian crustal dichotomy. *J. Geophys. Res.* 104:18981–90
- Weiss BP, Vali H, Baudenbacher FJ, Kirschvink

- JL, Stewart ST, Shuster DL. 2002. Records of an ancient Martian magnetic field in ALH84001. *Earth Planet. Sci. Lett.* 201: 449–63
- Wenzel MJ, Manga M, Jellinek AM. 2004. Tharsis as a consequence of Mars' dichotomy and layered mantle. *Geophys. Res. Lett.* 31: L04702
- Wieczorek MA, Zuber MT. 2004. Thickness of the Martian crust: improved constraints from geoid-to-topography ratios. *J. Geophys. Res.* 109:E01009
- Wieczorek MA, Phillips RJ. 2000. The "Procellarum KREEP Terrane": implications for mare volcanism and lunar evolution. *J. Geophys. Res.* 105:20417–30
- Wilhelms DE, Baldwin RJ. 1989. The role of igneous sills in shaping the Martian uplands. *Proc. Lunar Planet. Sci. Conf.* 19:355–65
- Wilhelms DE, Squyres SW. 1984. The Martian hemispheric dichotomy may be due to a giant impact. *Nature* 309:138–40
- Wilkins SJ, Schultz RA, Anderson RC, Dohm JM, Dawers NH. 2002. Deformation rates from faulting at the Tempe Terra extensional province, Mars. *Geophys. Res. Lett.* 29:1884
- Willemann RJ. 1984. Reorientation of planets with elastic lithospheres. *Icarus* 60:701–9
- Williams J-P, Nimmo F. 2004. Thermal evolution of the Martian core: implications for an early dynamo. *Geology* 32:97–100
- Wullner U, Harder H. 1998. Convection underneath a crust inhomogeneously enriched in heat sources: application to Martian mantle dynamics. *Phys. Earth Planet. Inter.* 109: 129–50
- Wyatt MB, McSween HY. 2002. Spectral evidence for weathered basalt as an alternative to andesite in the northern lowlands of Mars. *Nature* 417:263–66
- Wyatt MB, McSween HY, Tanaka KL, Head JW. 2004. Global geologic context for surface alteration on Mars. *Geology* 32:645–48
- Yuan DN, Sjogren WL, Konopliv AS, Kucinskis AB. 2001. Gravity field of Mars: a 75th degree and order model. *J. Geophys. Res.* 106:23377–3401
- Zhong S. 2002. Effects of lithosphere on the long-wavelength gravity anomalies and their implications for the formation of the Tharsis rise on Mars. *J. Geophys. Res.* 107:5054
- Zhong S, Zuber MT. 2001. Degree-1 mantle convection and the crustal dichotomy on Mars. *Earth Planet. Sci. Lett.* 189:75–84
- Zuber MT. 2001. The crust and mantle of Mars. *Nature* 412:220–27
- Zuber MT, Solomon SC, Phillips RJ, Smith DE, Tyler GL, et al. 2000. Internal structure and early thermal evolution of Mars from Mars Global Surveyor topography and gravity. *Science* 287:1788–93

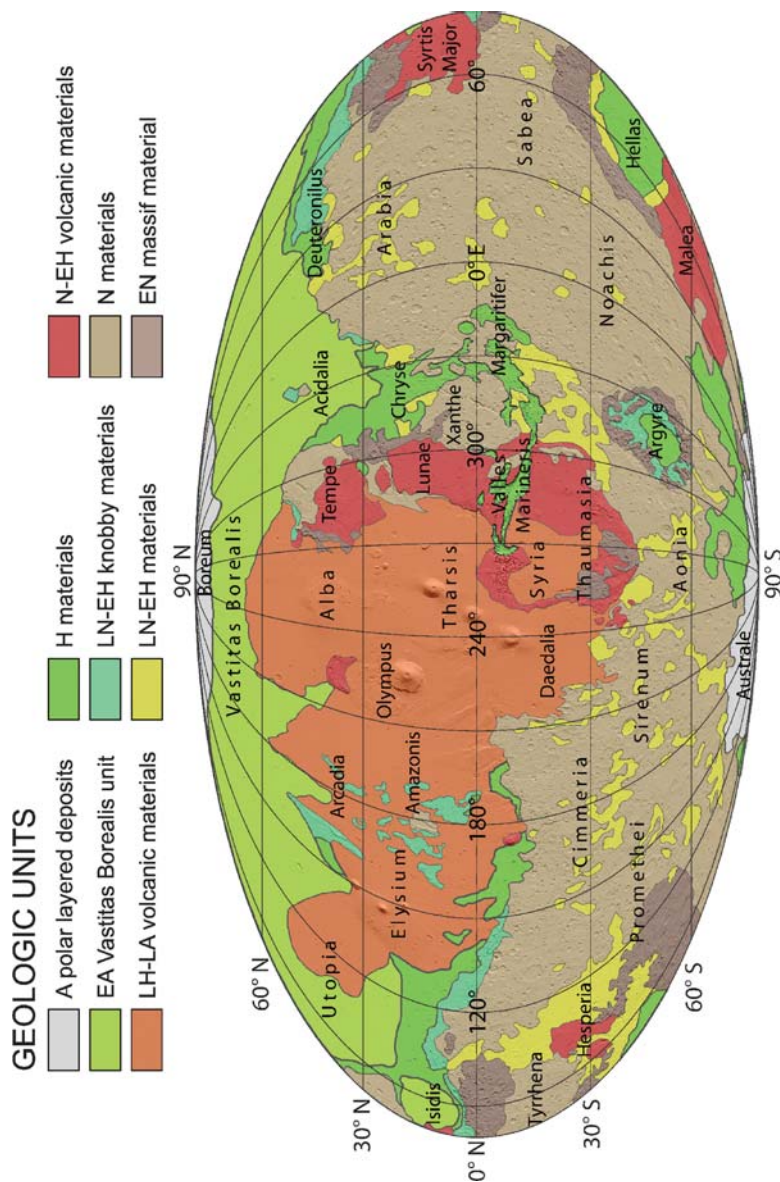


Figure 1 Generalized geologic map of Mars showing distribution of major material types as described in text. Unit age abbreviations: N, Noachian; H, Hesperian; A, Amazonian; E, Early; L, Late. Largely adapted from Scott et al. (1986–1987) and Tanaka et al. (2003b). Mollweide projection, using east longitudes, centered on 260°E, Mars Orbiter Laser Altimeter (MOLA) shaded-relief base illuminated from the East. On Mars, 1° latitude = 59 km.

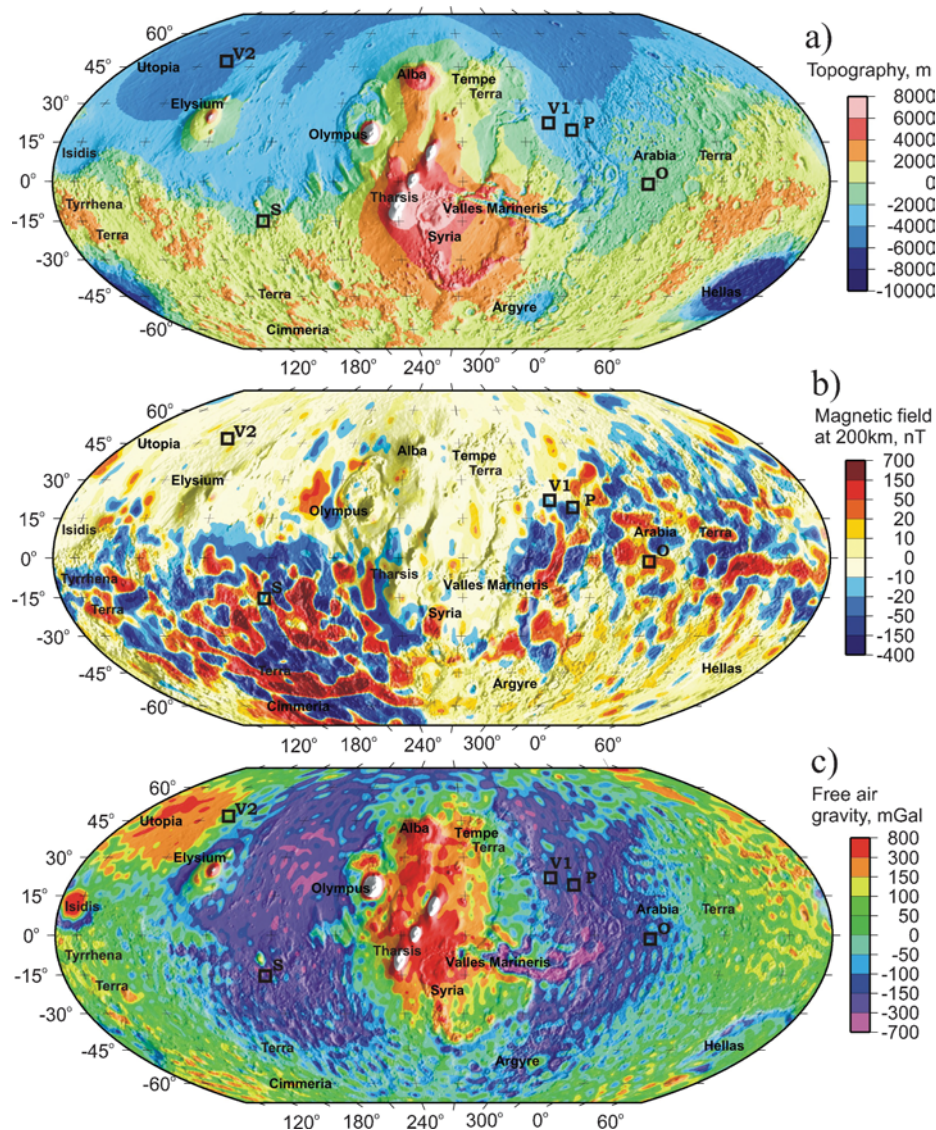


Figure 4 (A) MOLA topography, gridded at 0.25° intervals. Squares denote Mars lander locations: V indicates Vikings, P is Pathfinder, and S and O are the Spirit and Opportunity Mars rovers. (B) Radial magnetic field at 200 km, from Purucker et al. (2000), superimposed on shaded-relief topography. Note that contour scale is strongly nonlinear. Model uses 11,550 equally spaced dipoles to represent field. (C) Free-air gravity from model MGS75D (Yuan et al. 2001), evaluated to degree and order 75.